Hindawi
Journal of Combustion
Volume 2019, Article ID 2535073, 11 pages
https://doi.org/10.1155/2019/2535073

Research Article

Building Fire: Experimental and Numerical Studies on Behaviour of Flows at Opening

Philippe Onguene Mvogo,[1,2] Ruben Mouangue,[2,3] Justin Tégawendé Zaida,[4] Marcel Obounou,[5] and Henri Ekobena Fouda[2,3,5]

[1]*Department of Physics, Faculty of Sciences, University of Ngaoundere, Cameroon*
[2]*Laboratory of Analysis, Simulations and Experiments, University of Ngaoundere, Cameroon*
[3]*Department of Energy Engineering, IUT, University of Ngaoundere, Cameroon*
[4]*Department of Physics, University of Fada, Gourma Province, Burkina Faso*
[5]*Department of Physics, Faculty of Sciences, University of Yaounde 1, Cameroon*

Correspondence should be addressed to Ruben Mouangue; r_mouangue@yahoo.fr

Received 5 September 2018; Accepted 2 January 2019; Published 21 January 2019

Guest Editor: Cong-Ling Shi

Compartment fire is conducted by complex phenomena which have been the topics of many studies. During fire incident in a building, damage to occupants is not often due to the direct exposition to flames but to hot and toxic gases resulting from combustion between combustibles and surrounding air. Heat is therefore taken far from the source by combustion products which could involve a rapid spread of fire in the entire building. With the intention of studying the impact of the opening size on the behaviour of fire, experimental and computational studies have been undertaken in a reduced scale room including a single open door. Owing to Froude modelling, the obtained results have been transposed into full scale results. In accordance with experiments, numerical studies enabled the investigation of the influence of the ventilation factor on velocities of incoming air and outgoing burned gases and on areas of the surfaces crossed by these fluids during full-developed fire. Comparison of the deduced mass flow rates with the literature reveals an approval agreement.

1. Introduction

Compartment fires involve solid, liquid, or gaseous combustibles which burn in the presence of oxygen contained in surrounding air. Duration and heat release rate of fire depend on the type of combustible and on the ventilation level in compartment. Propagation of fire is strongly linked to the calorific energy released per unit time which consequently causes rise in temperature inside the room. Some complex phenomena happen while fire is ongoing among which the most dominant is the thermal plume defined as an upward flow of burned gases observed above the fire source. Fluid flow is governed by buoyancy forces induced by the difference of density between burned gases coming from combustion process and surrounding cool air [1]. Like other phenomena which could occur during compartment fire, the flashover phenomenon is the most dreaded by firemen during their intervention. It is defined as a rapid transition of fire from growth stage to violent full-developed fire during which all potential objects present in the room take part in combustion. Indeed, when the energy generated by fire source is greater than that lost through walls, the accumulation of heat inside the room provokes a rise in the temperature of burned gases located at ceiling. Once that temperature has exceeded a critical value of 600°C, a punctual and simultaneous ignition is produced, thus generalizing fire in the entire building [2].

The main characteristic of compartment fires is the relative lack of supply air which consequently makes prediction of the behaviour of fire difficult. According to some fire situations, flames will extinguish themselves or will lead to a catastrophic fire disaster. By applying the conservation law of energy inside the compartment, works have been done in the

past by authors. These works were mainly focused on some fire highlighting topics such as contribution of ventilation factor in building fire; research on the minimum heat release rate necessary to initialize the flashover; estimation of the energy lost through borders; and the contribution of the nature of walls material in fire [3–12]. All these studies, carried out theoretically, experimentally, or numerically by authors, intended to understand more mechanisms governing compartments fires and causing particular phenomena among which is the flashover phenomenon. All these studies underlined that the occurrence of flashover during an unexpected fire depends on several parameters such as the fire load inside compartment, calorific value of the combustible, size of the compartment, heat transfers and, the ventilation factor. The literature expresses the ventilation factor by the following mathematical expression: $W_o.H_o^{1.5}$ [9], where W_o and H_o represent the width and height of the opening, respectively. According to Chow [13], the likelihood of flashover to happen is high when certain main conditions are combined among which are a minimum heat flux at floor of 20 kW/m^2, a minimum fuel burning rate of 40-80 g/s, and a critical temperature of burned gases of 600°C.

Focusing on these anterior works, mechanisms controlling compartment fires are multiple but the main factor is the ventilation level which depends on the size of opening (s). Behaviour of fire inside a compartment will then depend both on the airflow entrained in the room in fire and on the burned gases out coming from the room. Owing to experimental tests enabling us to validate the CFD studies (Computational Fluid Dynamics), the present paper aims to study numerically the sensitivity of the fluids flow at the opening when the ventilation factor is varying during compartment fire. So, for different width values of the opening, experiments and then simulations are carried out in view of bringing out the velocity and the area of the surface crossed by exterior air and interior burned gases.

1.1. Froude Similarity Modelling. Fire tests performing on full scale models would ideally accurate predictions of fire behaviour but it is very expensive, time consuming, and very dangerous to conduct full scale fire tests. Owing to the dimensionless groups derived from the governing differential equations, Quintiere [14] has examined the principles for scaling fire phenomena; several scaling techniques have been described and illustrated. Among these methods, Froude modelling has been exploited by authors to conduct fire experiments using a small geometric model [15–20]. This approach is applied in compartment fire situations because of the fact that convective flows are dominant to diffusive flows. Froude number, which represents the ratio of inertia force to gravitational force, is the dimensionless parameter which is preserved between both scales (Equation (1)). The scaling relationships giving the velocity V and the heat release rate $\dot{Q}$ are presented by Equations (2) and (3), respectively. L represents the characteristic length of the domain and g the acceleration of the gravity:

$$F_r = \frac{V^2}{gL} \tag{1}$$

$$\left(\frac{V}{\sqrt{L}}\right)_{Small\ scale} = \left(\frac{V}{\sqrt{L}}\right)_{Full\ scale} \tag{2}$$

$$\left(\frac{\dot{Q}}{L^{5/2}}\right)_{Small\ scale} = \left(\frac{\dot{Q}}{L^{5/2}}\right)_{Full\ scale} \tag{3}$$

1.2. Mass Flow Rates of Fluids at Opening. In compartment fire, ambient cool air is entrained in the compartment through the lower portion of the opening. The mass flow rate of that entrained air has been assumed to be given by the expression of Prahl and Emmons [21] ameliorated later by Zukoski *et al.* [22] (Equation (4)). Hot smoke would flow out of the compartment through the upper portion of the opening. Driven by buoyancy flow, the mass flow rate of burned gases out coming from the opening has been assumed to be given by the expression of Rockett [23] (Equation (5)):

$$\dot{m}_{in} = 0.50 A_0 \sqrt{H_0} \tag{4}$$

$$\dot{m}_{out} = \frac{2}{3} \cdot C_d \rho_0 W_0 {H_0}^{3/2} \sqrt{2g\left(1 - \frac{Z_N}{H_0}\right)\frac{T_0}{T_g}\left(1 - \frac{T_0}{T_g}\right)}\left(1 - \frac{Z_N}{H_0}\right) \tag{5}$$

Where C_d is the flow coefficient, Z_N is the height of discontinuity between hot gases layer and cool air layer, W_0 and H_0 are the width and height of the opening, respectively, and T_g and T_0 represent the temperature of hot gases and ambient cool air, respectively.

2. Material and Methods

2.1. Experimental Set-Up. Inspired from the works of Sahu *et al.* [24], fire experiments were performed in a one-fifth scale compartment of inner dimensions: 0.50 m x 0.50 m x 0.50 m, which included an open door of dimensions 0.20 m x 0.40 m ($W_0 \times H_0$) at the front wall (Figure 1). Walls and ceiling of the model were made out from lightweight concrete with a thickness of 15 mm and of which the density and thermal conductivity are worth 800 kg/m^3 and 0.20 W/mK, respectively. Located at the center of floor, the fire source was a cylindrical pan of diameter 0.13 m, in which a mass of 0.065 kg of diesel fuel has been introduced of which the average calorific value is worth 43.4 MJ/kg. This latter represented the fire load of experiments. Temperature of hot gases inside the compartment was automatically recorded using the data acquisition/switch unit Agilent-34970A (Figure 2(a)) through an array of fifteen N-type thermocouples (Figure 2(b)) installed inside the domain and at the inner side of the opening. The locations of these sensors are given in Table 1. Temperatures of the outgoing gases, flames, and the exterior surfaces were measured using the devices presented in Figures 2(c), 2(d), and 2(e). Experimental protocol consisted of igniting the fire source and then performing measurements till the fuel is completely burned. In

Table 1: Locations of thermocouples in the experimental room.

Thermocouple	x [m]	y [m]	z [m]
T1	0.35	0.06	0.06
T2	0.35	0.06	0.12
T3	0.35	0.06	0.17
T4	0.35	0.06	0.22
T5	0.35	0.06	0.27
T6	0.35	0.06	0.32
T7	0.35	0.06	0.37
T8	0.35	0.06	0.41
T10	0.48	0.22	0.10
T15	0.48	0.22	0.15
T20	0.48	0.22	0.20
T25	0.48	0.22	0.25
T30	0.48	0.22	0.30
T35	0.48	0.22	0.35
T39	0.48	0.22	0.39

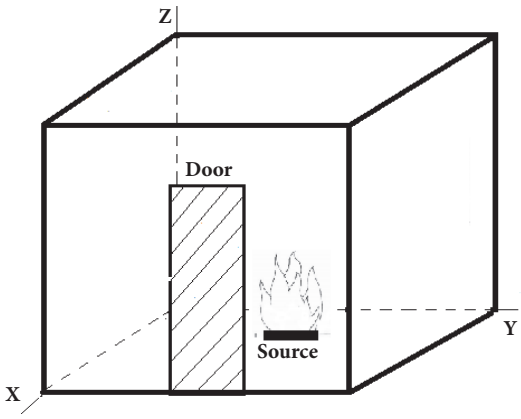

Figure 1: Experimental domain of dimensions 0.50 m x 0.50 m x 0.50 m including in its front wall a single open door of dimensions 0.20 m x 0.40 m.

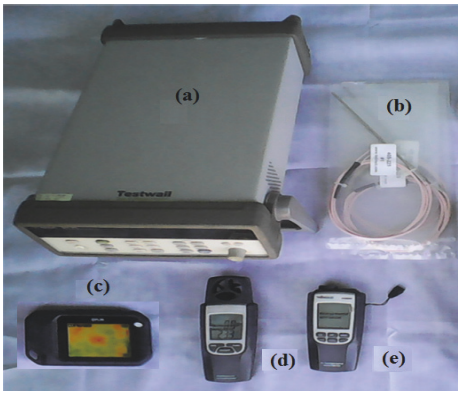

Figure 2: Measuring devices: (a) data acquisition/switch unit enabling us to automatically record measurements during the fire test following a time step (Agilent-34970A); (b) thermocouples of type N: range: [-100...1300]±1°C; (c) infrared camera (FLIR C2): range: [–10...150]±2°C; (d) thermoanemometer; (e) infrared thermometer (Velleman): range: [-50...300]±3°C.

view of studying the influence of the ventilation factor on the fire behaviour, a sliding door enabling us to modify the door's width has been used. Thus, four values of width have been used (0.20 m, 0.15 m, 0.10 m, and 0.075 m) corresponding to four fire scenes to be experimented and simulated. In view of checking the repeatability and accuracy of experiments, each fire experiment has been repeated three times and only the average values were exploited and interpreted.

Compartment fires are different from fire occurring in the open air because of the room walls. Fire development is generally characterized in terms of heat release rate which represents the heat produced per unit time $\dot{Q}$. It is calculated using the expression given Equation (6) [13], where χ is the combustion efficiency generally found within 0.7 and 0.9 and $\Delta H_{c,eff}$ is the effective heat of combustion:

$$\dot{Q} = \chi \dot{m} \Delta H_{c,eff} \quad (6)$$

The term $\dot{m}$ represents the fuel mass loss during fire, which is commonly deduced using a load cell during experiment. But, as that device was not available at the moment the present work was ongoing, the mass loss rate has been determined using the regression velocity which represents the burning rate of fuel ν (Equation (7)) [6]. The term t_b expresses the burning duration of combustible and, as the fire source is a liquid fuel contained in a pan, the pool fuel diameter remains constant during the full developed fire and, knowing that the mass loss has a t-square curve during growth and decay phases, the burning duration will be the time prompt at the end of the full development phase so as to better approximate the real mass loss rate. The mass loss rate during decay phase is then assumed to compensate for the mass loss rate during growth phase. So, for a fixed volume of fuel W put inside a

Table 2: Numerical modelling of experiments.

Physical concept	Model
Combustion	EDC concept (z, Y_F)
Turbulence	Standard $k-\varepsilon$ ($k=\varepsilon=10^{-3}$)
Radiation	P1-approximation ($\epsilon=0.41$) [23]
Boundary conditions	Convection-conduction (ρ, λ)
Space and time step	Concept of Courant-Friedrichs-Lewy (CFL)

pan of diameter D, the mass loss rate of fuel $\dot{m}$ is calculated using the expression given by Equation (8). Terms ρ_f and A_f represent the density and the pool area of fuel, respectively:

$$\nu = \frac{4W}{\pi D^2 t_b} \tag{7}$$

$$\dot{m} = \rho_f A_f \nu \tag{8}$$

2.2. Numerical Modelling

2.2.1. Modelling of Fire Phenomenon. CFD modelling is a numerical approach which allows the prediction of various aspects of thermal fluid phenomena [25]. The use of this method involves a mathematical description of physical and chemical processes associated with the physical reality. Equations governing fluid flow are obtained by applying the principles of mass conservation (Equation (9)), momentum conservation (Equation (10)), energy conservation (Equation (11)), species conservation (Equation (12)), and state law (Equation (13)). These equations are treated and solved numerically within a finite domain. Numerical methods are widely used by the scientific community; in the field of fire safety, many fire models have been established [26–29]:

$$\frac{\partial \rho}{\partial t} + \nabla \bullet \left(\rho \vec{u}\right) = 0 \tag{9}$$

$$\frac{\partial}{\partial t}\left(\rho \vec{u}\right) + \nabla \bullet \left(\rho \vec{u} \otimes \vec{u}\right) = -\nabla P + \nabla \bullet \overline{\overline{\tau}} + \left(\rho - \rho_0\right)\vec{g} \tag{10}$$

$$\frac{\partial}{\partial t}\left(\rho h\right) + \nabla \bullet \left(\rho \vec{u} h\right) = \frac{dP}{dt} + \nabla \bullet \left(\frac{\lambda}{C_p}\nabla h - q_r\right) + Q_{ext} \tag{11}$$

$$\frac{\partial}{\partial t}\left(\rho Y_k\right) + \nabla \bullet \left(\rho \vec{u} Y_k\right) = \nabla \bullet \left(\rho D_k \nabla Y_k\right) + \rho \dot{w}_k \tag{12}$$

$$P = \rho \frac{R}{M} T \tag{13}$$

2.2.2. Numerical Code. Numerical simulations are conducted using the CFD code ISIS 4.2.1 [30–32]. Developed by the Institute of Radioprotection and Nuclear Safety (IRSN) [30], ISIS is an open source code dedicated to the fire-driven fluid flow and especially to the numerical simulation of fire in open and confined environment. It can be associated with other processing tools such as Gmsh and Paraview which are used in the present study for geometry building and postprocessing, respectively. Accuracy of solution provided by simulation may be affected by many factors such as the adoption of submodels describing the complex physical and chemical processes (combustion, turbulence, radiation etc.), density of the discretization grid, and specification of initial boundaries conditions. Table 2 summarizes the numerical modelling applied to design experiments.

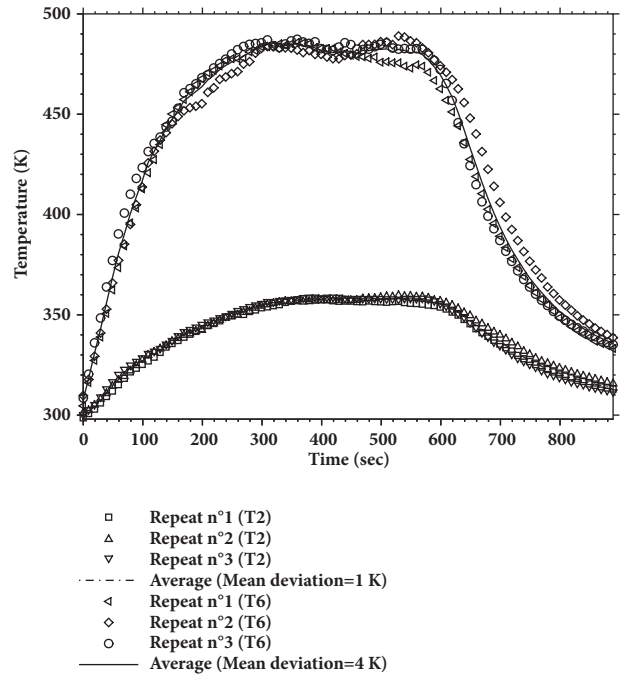

Figure 3: Illustration of the repeatability of experiments: close to the ceiling (T6) and near the floor (T2), the average errors of temperature are 4K and 1K, respectively.

3. Results and Discussion

3.1. Experimental Results

3.1.1. Repeatability of Experiments. In view of bringing out the repeatability of experiments, being undertaken under the same experimental conditions, each fire scene has been repeated three times. The repeated profiles of temperature of two chosen thermocouples (T2 and T6) are presented in Figure 3. It can be observed that the scatter of data is almost similar and recurs with acceptable mean deviation. The three

Table 3: Burning duration and mass loss rate of tests according to the ventilation factor.

	H_o [m]	W_o [m]	$W_oH_o^{1.5}$ [$m^{5/2}$]	t_b [sec.]	ν [$\times10^{-5}$ m/s]	$\dot{m}$ [$\times10^{-4}$ kg/s]
Scene 1	0.40	0.20	0.051	570	1.0579	1.1517
Scene 2	0.40	0.15	0.038	530	1.1378	1.2386
Scene 3	0.40	0.10	0.025	490	1.2307	1.3397
Scene 4	0.40	0.075	0.019	540	1.1167	1.2157

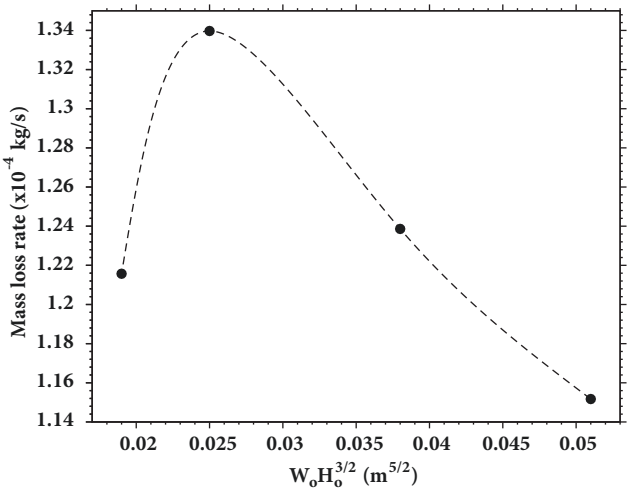

Figure 4: Influence of the variation of ventilation factor on the fuel burning rate.

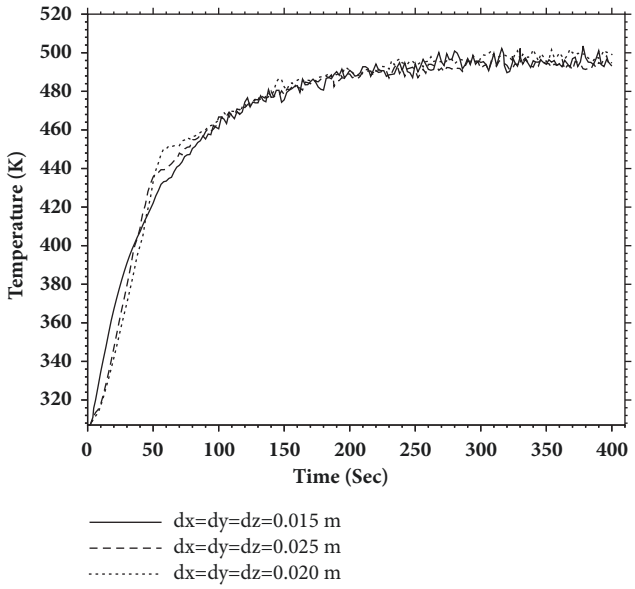

Figure 5: Sensitivity study of grid size.

phases of a fire incident are clearly pointed up and where the fire growth starts from the ignition to time t=300s while the full developed fire begins from 300s to 600s. Decay phase begins at t=600s till the flame is completely extinguished.

3.1.2. Influence on the Fuel Burning Rate. The mass loss rate of each fire scene is deduced owing to the burning duration and regression velocity (Table 3). In Figure 4, showing the variation of the mass loss rate according to the ventilation factor, it can be noticed that, when the ventilation factor is between $0.02m^{5/2}$ and $0.025m^{5/2}$, the fuel burning rate is increasing till reaching a peak value of $1.3397x10^{-4}$ kg/s but from $0.025m^{5/2}$ to $0.051m^{5/2}$ the fuel burning rate remains decreasing tending to reach a constant value representing the mass loss rate in an open environment. This change in the variation direction of the mass loss rate is due to the passing of fire from the ventilation-controlled fire to the fuel-controlled fire. Indeed, energy released by fire is then closely linked to the quality of combustion which depends on the air supplying the source. So, the more the door is opened the more the airflow entrained in the room is important. Transition from the ventilation-controlled fire to the fuel-controlled fire depends mainly on the size of the fire source compared to the size of compartment as well as the size of its opening (s).

3.2. Numerical Results

3.2.1. Grid-Sensitivity Study. In view of better approximating a real fire incident, sensitivity study of grid size is necessary. Several past studies stated that a grid-sensitivity analysis should be conducted in order to ensure that results will not be influenced by the grid size [33, 34]. After the numerical modelling, different grid sizes (0.015m, 0.020m, and 0.025m) have been used to test its influence on results. Figure 5 presents the temperature evolution of hot gases (T8) computed with different space steps. It can then be observed that there is not significant change on curves; it is the reason why all the simulations have been performed using 0.025m as space step.

3.2.2. Verification and Validation of Results. Figures 6(a), 6(b), 6(c), and 6(d) represent, for each fire case, the confrontation between experimental and numerical profiles of temperature along the height of the door, plotted during the steady state precisely at time t=400 seconds. The difference observed between simulation and experiment is due to the fact that compartment fire is governed by high turbulent flows which could not be exactly simulated; it is the reason why the standard k-epsilon model is used in order to approximate the real fire situation. Although not having the same trajectory, it is however noticed that both experimental and numerical curves almost have a similar behaviour. So, there is an acceptable approval between experiment and simulation. Analysis of these results enabled us to notice that two zones

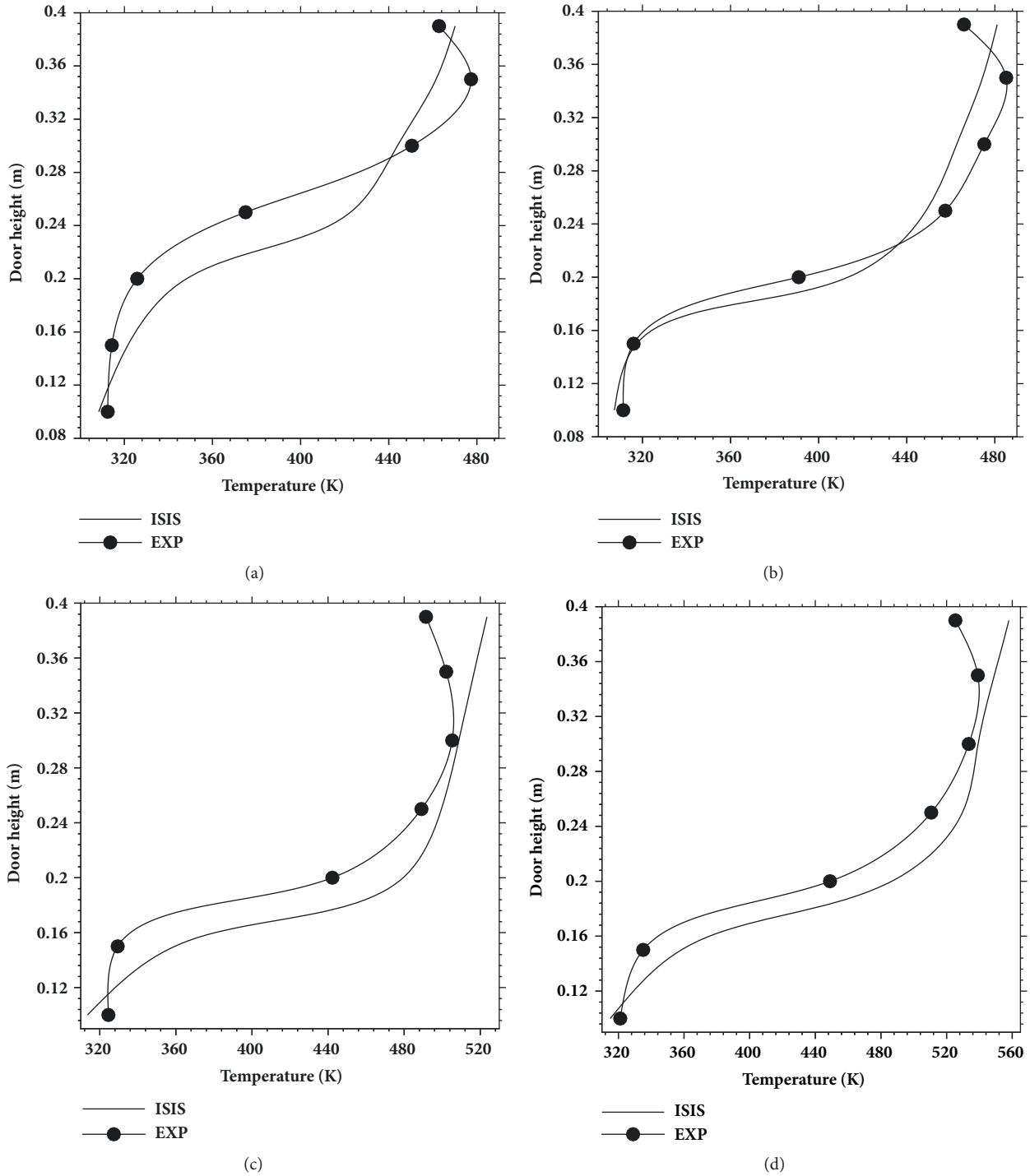

Figure 6: Profiles of temperature at the door during the full developed fire, at time t=400sec. (a) Scene 1: W_0=0.20 m. (b) Scene 2: W_0=0.15 m. (c) Scene 3: W_0=0.10 m. (d) Scene 4: W_0=0.075 m.

of the opening are put forward: a lower zone which is crossed by incoming air supplying the fire source and an upper zone which is crossed by outgoing hot gases. The neutral zone, characterized by a rough change in temperature, represents the interface zone between the hot gases layer and the cool air layer.

3.2.3. Velocities Fields at the Door. Also captured during the steady state (t=400 sec), Figure 7 presents the velocities fields at the front wall including the door. On contours of the door, the two mentioned zones are well visualized. Represented by negative velocities values, the exterior ambient air enters the compartment through the lower portion of the door while the

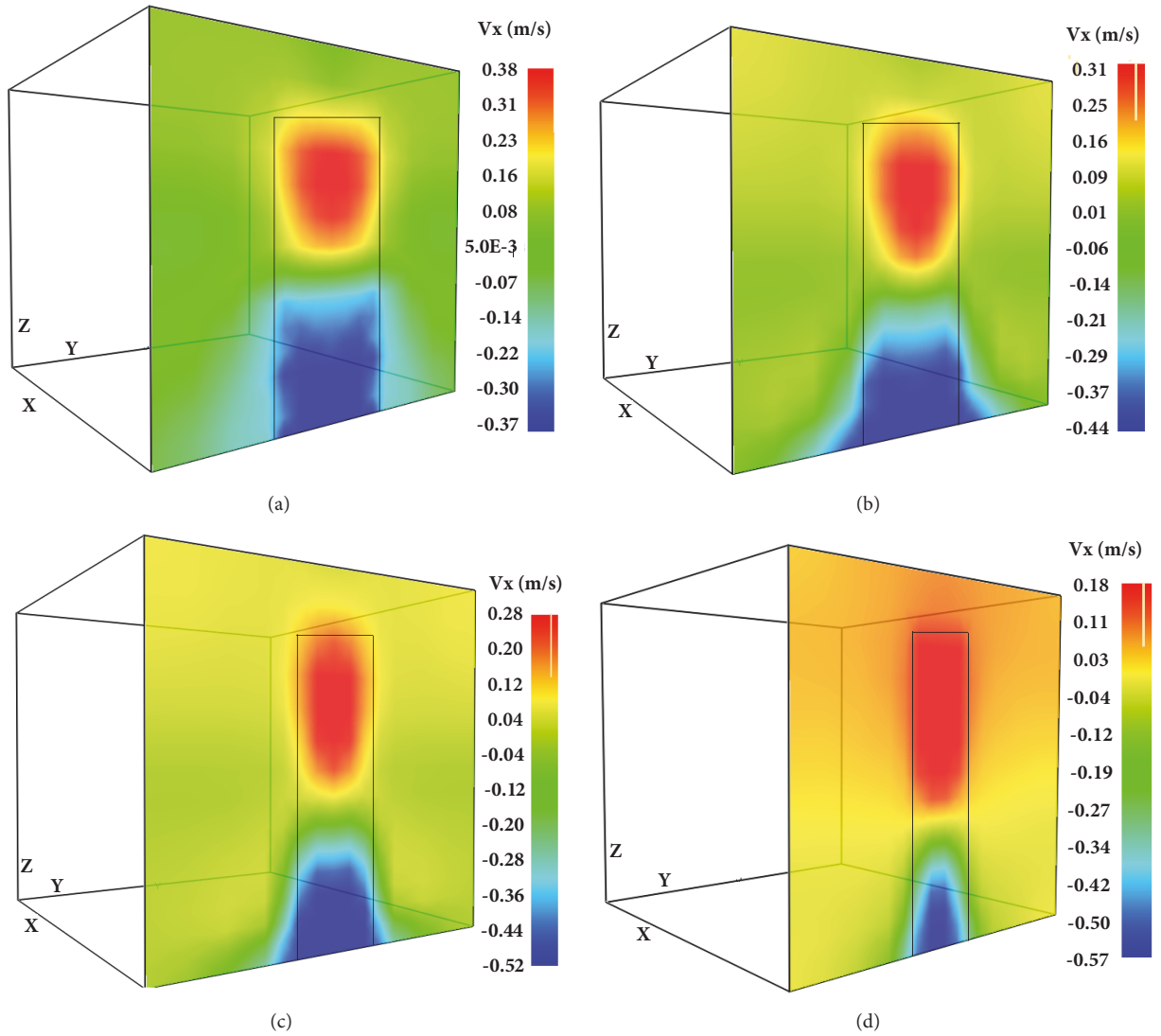

FIGURE 7: Contours of velocities at the door during the full developed fire, at time t=400sec. (a) Scene 1: W_0=0.20 m. (b) Scene 2: W_0=0.15 m. (c) Scene 3: W_0=0.10 m. (d) Scene 4: W_0=0.075 m.

burned gases, represented by positive velocities values, go out through the upper portion of the door.

For each fire scene, only the maximal values of the incoming velocity of air (V_{in}) and outgoing velocity of gases(V_{out}) are exploited. Heights occupied by these crossing fluids are deduced using the vertical profiles of velocity at the door (Figure 8). In fact, a projection of the zero-value velocity on curve enables us to estimate the height of incoming air layer (H_{in}). Height crossed by burned gases layer (H_{out}) is simply deduced by a subtraction to the door height. All these different values of heights and velocities are reported in Table 4.

Applying the Froude modelling, these reduced scale results are converted into full scale results representing a real fire incident occurring in a full scale compartment of dimensions 2.50 m x 2.50 m x 2.50 m which includes an open door of dimensions 1.0 m x 2.0 m. Table 5 presents the general full scale parameters searched in this study such as the heat release rate of each fire scene, the maximal velocity, the area of the crossed portion of the door, and the mass flow rate of the incoming or outgoing fluid.

Plotting of data in Table 5 enabled us to illustrate the variation of some parameters according to the ventilation factor. Concerning particularly the incoming ambient air, it is obviously noticed that both the velocity (Figure 9) and the area of the crossed portion of door (Figure 10) are inversely proportional to the ventilation factor. Indeed while the velocity decreases the area of the portion of door crossed by cool air increases.

On the other hand, results revealed that hot gases flowing out from the compartment behave differently compared to the incoming cool air. It shows that the velocity and the area of the crossed portion of door evolve proportionally to the ventilation factor. The more the door is opened the more these both parameters increase.

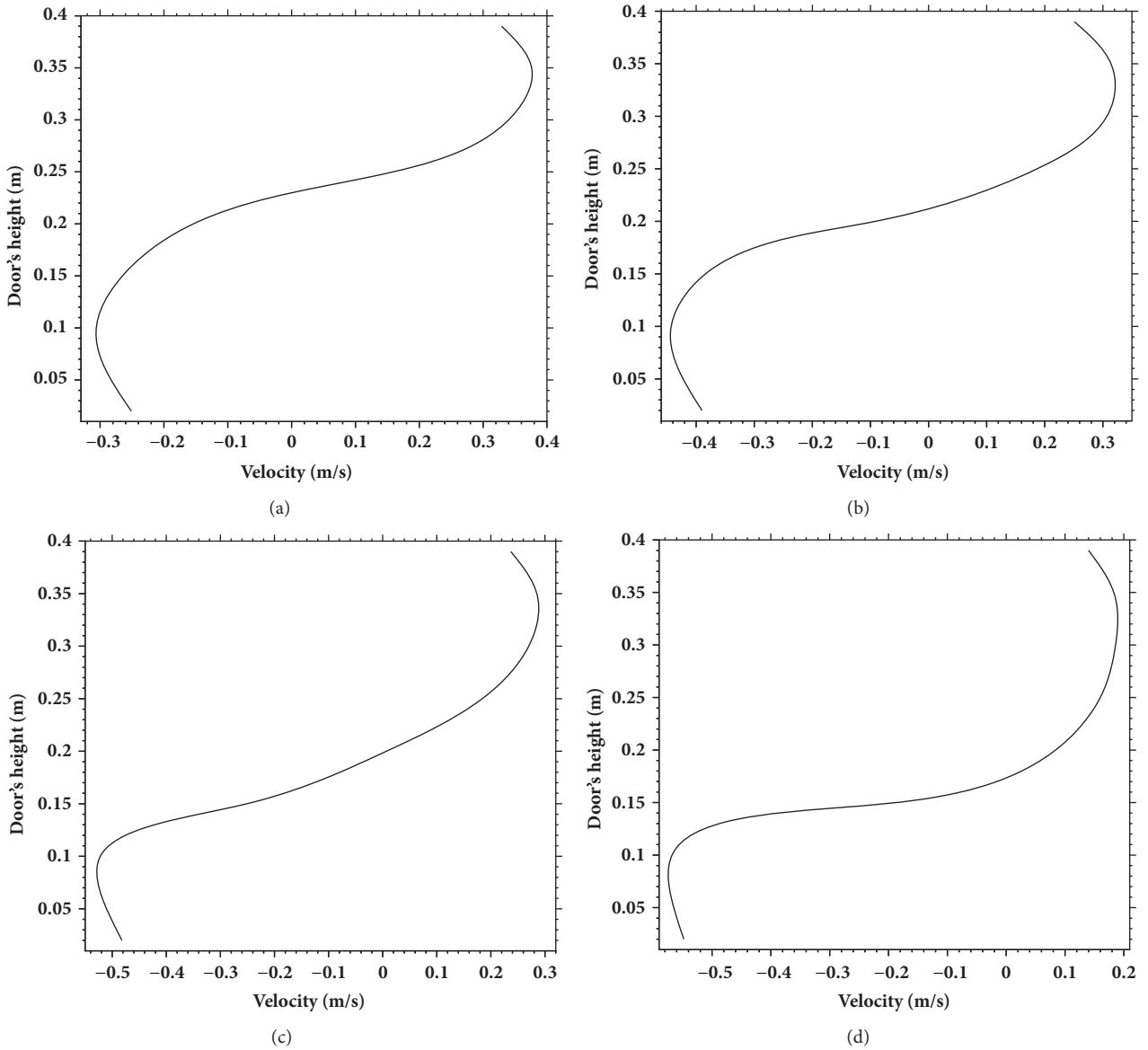

Figure 8: Vertical profiles of velocity at the door during the full developed fire, precisely at time t=400s. (a) Scene 1: W_0=0.20 m. (b) Scene 2: W_0=0.15 m. (c) Scene 3: W_0=0.10 m. (d) Scene 4: W_0=0.075 m.

Table 4: Heights and maximal velocities of fluids at door in small scale.

Scene n°	$W_0 H_0^{3/2}$ [$m^{5/2}$]	$\dot{Q}$ [kW]	H_{in} [m]	V_{in} [m/s]	H_{out} [m]	V_{out} [m/s]
Scene 1	0.051	4.14	0.15	0.37	0.17	0.38
Scene 2	0.038	4.50	0.18	0.44	0.20	0.31
Scene 3	0.025	4.82	0.20	0.52	0.22	0.28
Scene 4	0.019	4.38	0.23	0.57	0.25	0.18

Indeed, buoyancy forces generated in the fire plume are at the origin of the raising of velocity of outgoing gases. The more the opening's width is wide the more the convective flow is prevailing. The convective mixing induced at ceiling raises the kinetic motion of hot gases; this is the reason why they flow out with high velocity in spite of the expansion of the crossed surface.

After having simulated the velocity and the surface area crossed by the fluid, the mass flow rate is calculated assuming the density of fluid equal to 1.25 kg/m^3. Comparison of

Table 5: Results of the behaviour of incoming and outgoing fluids at door in full scale.

Scene n°	$W_0 H_0^{3/2}$ [$m^{5/2}$]	$\dot{Q}$ [kW]	V_{in} [m/s]	A_{in} [m^2]	$\dot{m}_{in}$ [kg/s]	V_{out} [m/s]	A_{out} [m^2]	$\dot{m}_{out}$ [kg/s]
Scene 1	2.83	231.43	0.830	1.15	1.189	0.849	0.850	0.903
Scene 2	2.12	251.55	0.984	0.75	0.922	0.693	0.750	0.650
Scene 3	1.42	269.44	1.163	0.45	0.654	0.630	0.550	0.430
Scene 4	0.70	244.84	1.275	0.28	0.448	0.402	0.469	0.236

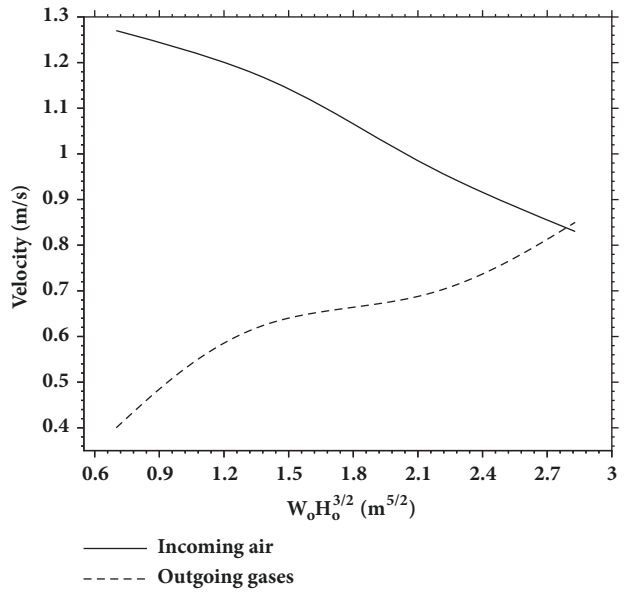

Figure 9: Variation of velocities of cool air and hot gases over ventilation factor.

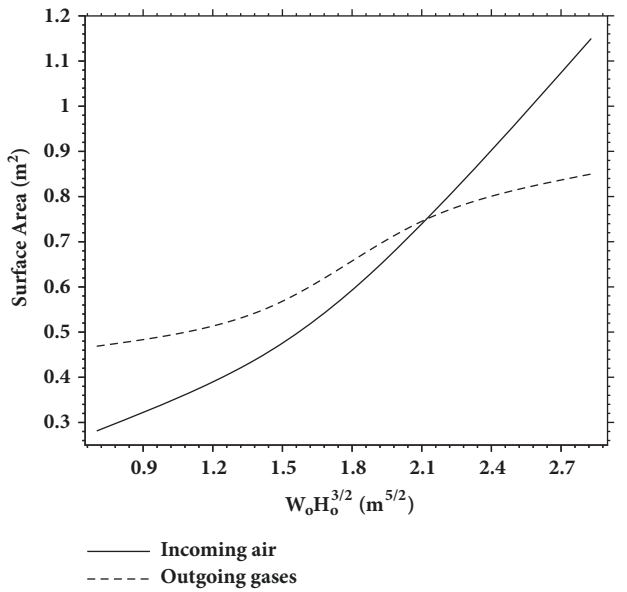

Figure 10: Variation of surface areas crossed by cool air and hot gases over ventilation factor.

these calculated mass flow rates to those of the literature allows us to reveal an approval agreement between results (Figures 11 and 12). These Figures illustrate the variation of the mass flow rates of incoming air and outgoing burned gases compared to results obtained by Zukoski et al. [22] and Rockett [23], respectively. The error observed between the calculated and the literature curve is certainly due to the numerical modelling which can rather be improved by operating on the initial and boundaries conditions.

4. Conclusion

Compartment fire is generally held according to three phases of which are growth, full development, and decay. During these phases, dangerous phenomena may occur and lead to catastrophic situation in which human and material damage could be reported. This paper aimed at studying the influence of the ventilation factor on the behaviour of fluids at the door during a single-opening compartment fire. Owing to experiments and CFD simulations, details concerning the velocity and crossed surface of incoming air and outgoing smokes were brought out. Future works will be to perform more simulations with more width values in view of establishing mathematical relations.

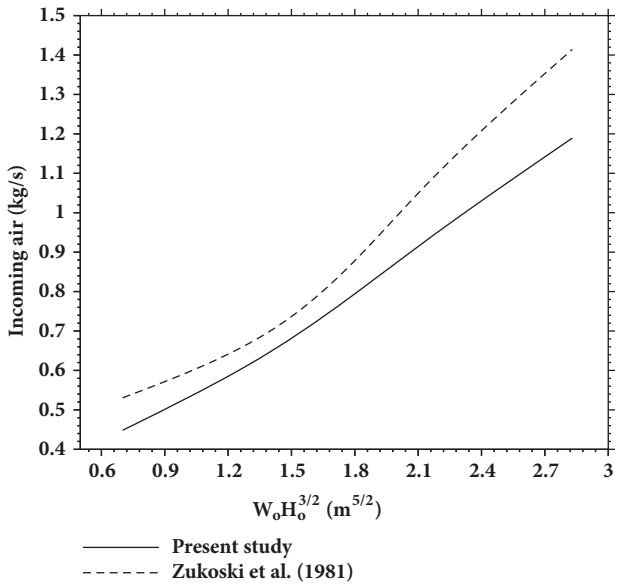

Figure 11: Variation of the mass flow rate of incoming air over ventilation factor (full scale).

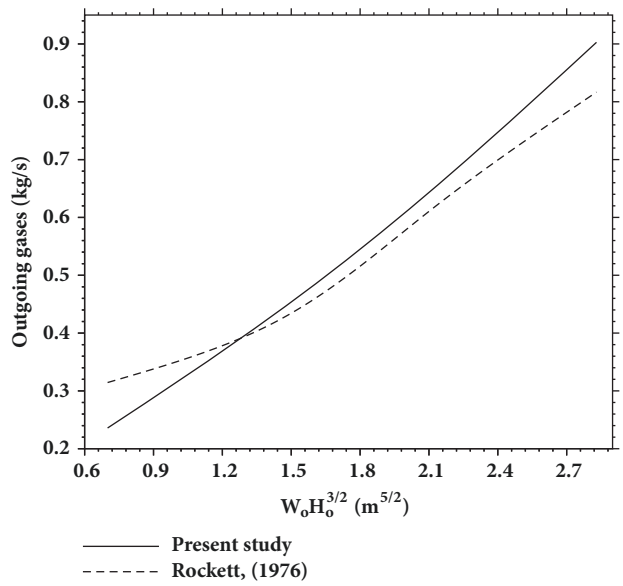

Figure 12: Variation of the mass flow rate of outgoing gases over ventilation factor (full scale).

Symbols

L:	Characteristic length (m)
V:	Characteristic velocity (m/s)
$\Delta H_{c,eff}$:	Effective heat of combustion (kJ/kg)
H:	Height of compartment (m)
$\dot{m}$:	Mass loss rate of fuel (kg/s)
A_f:	Pool fuel area (m^2)
D:	Pool fuel diameter (m)
T_g:	Temperature of hot gases (K)
T_0:	Temperature of cool air (K)
V_{out}:	Maximal velocity of outgoing gases (m/s)
V_{in}:	Maximal velocity of incoming air (m/s)
χ:	Combustion efficiency (0.8)
t_b:	Average fire duration (s)
λ:	Thermal conductivity of the wall (W/m.K)
z:	Mixture fraction of fuel with air (.)
ϵ:	Emissivity of hot gases in the enclosure (.)
ν:	Regression velocity (m/s)
W_o:	Width of opening (m)
H_o:	Height of opening (m)
ρ_f:	Density of fuel (kg/m^3)
W:	Initial volume of fuel (m^3)
C_d:	Flow coefficient (0.7)
Z_N:	Height of discontinuity (m)
H_{in}:	Height crossed by cool air (m)
H_{out}:	Height crossed by smoke (m)
A_{in}:	Area crossed by cool air (m^2)
A_{out}:	Area crossed by cool air (m^2)
$\dot{m}_{in}$:	Mass flow rate of cool air (kg/s)
$\dot{m}_{out}$:	Mass flow rate of smoke (kg/s)
k:	Kinetic turbulent energy (m^2/s^2)
ε:	Dissipation rate of turbunce (m^2/s^3)
Y_F:	Mass fraction of fuel (.).

Data Availability

The data used to support the findings of this study are available from the corresponding author upon request.

Conflicts of Interest

The authors declare that they have no conflicts of interest.

References

[1] G. Heskestad, "Fires plumes, flame height and air entrainment," in *Handbook of Fire Protection Engineering*, Chapter 1, Section 2, 3rd edition, 2003.

[2] T. Breton and Y. Duthen, "Simulations of Fire Propagation in Urban Environment," 40 pages, hal-00287987, 2008.

[3] V. Babrauskas, "Estimating room flashover potential," *Fire Technology*, vol. 16, no. 2, pp. 94–103, 1980.

[4] B. J. McCaffrey, J. G. Quintiere, and M. F. Harkleroad, "Estimating room temperatures and the likelihood of flashover using fire test data correlations," *Fire Technology*, vol. 17, no. 2, pp. 98–119, 1981.

[5] P. H. Thomas, "Testing products and materials for their contribution to flashover in rooms," *Fire and Materials*, vol. 5, no. 3, pp. 103–111, 1981.

[6] V. Babrauskas, "Free burning fires," *Fire Safety Journal*, vol. 11, no. 1-2, pp. 33–51, 1986.

[7] S. R. Bishop, P. G. Holborn, A. N. Beard, and D. D. Drysdale, "Nonlinear dynamics of flashover in compartment fires," *Fire Safety Journal*, vol. 21, no. 1, pp. 11–45, 1993.

[8] T. L. Graham, G. M. Makhviladze, and J. P. Roberts, "Flashover sands the effects of compartment scale," *Applied Fire Science*, vol. 17, pp. 115–128, 1998.

[9] R. Huo, X. H. Jin, C. L. Shi, and W. K. Chow, "On the equation of flashover fire in small compartments," *International Journal of Engineering Performance-Based Fire Codes*, vol. 3, pp. 158–165, 2001.

[10] J. Zehfuss and D. Hosser, "A parametric natural fire model for the structural fire design of multi-storey buildings," *Fire Safety Journal*, vol. 42, no. 2, pp. 115–126, 2007.

[11] A. N. Beard, "Flashover and boundary properties," *Fire Safety Journal*, vol. 45, no. 2, pp. 116–121, 2010.

[12] A. Chen, S. Yang, and X. Dong, "Studies of the combined effects of some important factors on the likelihood of flashover," *Fire and Materials*, vol. 35, no. 2, pp. 105–114, 2011.

[13] W. K. Chow, "New inspection criteria for flashover in compartmental fires," *Fire and Materials*, vol. 23, no. 1, pp. 13–15, 1999.

[14] J. G. Quintiere, "Scaling applications in fire research," *Fire Safety Journal*, vol. 15, no. 1, pp. 3–29, 1989.

[15] H. Takeda, "Small-scale experiments of flame spread in preflashover compartment fires," *Fire and Materials*, vol. 9, no. 1, pp. 36–40, 1985.

[16] S. Jolly and K. Saito, "Scale modeling of fires with emphasis on room flashover phenomenon," *Fire Safety Journal*, vol. 18, no. 2, pp. 139–182, 1992.

[17] R. O. Carvel, A. N. Beard, and P. W. Jowitt, "The influence of longitudinal ventilation systems on fires in tunnels," *Tunnelling and Underground Space Technology*, vol. 16, no. 1, pp. 3–21, 2001.

[18] C. C. Hwang and J. C. Edwards, "The critical ventilation velocity in tunnel fires—a computer simulation," *Fire Safety Journal*, vol. 40, no. 3, pp. 213–244, 2005.

[19] G. H. Ko, S. R. Kim, and H. S. Ryou, "An Experimental Study on the Effect of Slope on the Critical Velocity in Tunnels," *Journal of Fire Sciences*, vol. 28, pp. 27–46, 2010.

[20] R. Mouangue, P. M. Onguene, J. T. Zaida, and H. P. F. Ekobena, "Numerical Investigation of Critical Velocity in Reduced Scale Tunnel Fire with Constant Heat Release Rate," *Journal of Combustion*, vol. 2017, Article ID 7125237, 12 pages, 2017.

[21] J. Prahl and H. W. Emmons, "Fire induced flow through an opening," *Combustion and Flame*, vol. 25, pp. 369–385, 1975.

[22] E. E. Zukoski, T. Kubota, and B. Cetegen, "Entrainment in fire plumes," *Fire Safety Journal*, vol. 3, no. 3, pp. 107–121, 1981.

[23] J. A. Rockett, "Fire Induced Gas Flow in an Enclosure," *Combustion Science and Technology*, vol. 12, no. 4-6, pp. 165–175, 1976.

[24] D. Sahu, S. Kumar, S. Jain, and A. Gupta, "Full scale experimental and numerical studies on effect of ventilation in an enclosure diesel pool fire," *Building Simulation*, vol. 10, pp. 351–364, 2017.

[25] J. Anderson, *Computational Fluid Dynamics: The Basics with Applications*, McGraw-Hill, New York, NY, USA, 1995.

[26] R. Friedman, "An International Survey of Computer Models for Fire and Smoke," *Journal of Fire Protection Engineering*, vol. 4, no. 3, pp. 81–92, 1992.

[27] A. M. Hasofer and V. R. Beck, "A stochastic model for compartment fires," *Fire Safety Journal*, vol. 28, no. 3, pp. 207–225, 1997.

[28] R. D. Peacock, P. A. Reneke, C. L. Forney, and M. M. Kostreva, "Issues in Evaluation of Complex Fire Models," *Fire Safety Journal*, vol. 30, no. 2, pp. 103–136, 1998.

[29] L. Kerrison, E. R. Galea, and M. K. Patel, "A Two-dimensional Numerical Investigation of the Oscillatory Flow Behaviour in Rectangular Fire Compartments with a Single Horizontal Ceiling Vent," *Fire Safety Journal*, vol. 30, no. 4, pp. 357–382, 1998.

[30] IRSN, "Documentation on the physical modelling in ISIS, France," 2008, WzmGCNUzbDc, 2008, http://www.irsn.fr/FR/Larecherche/outils-scientifiques/Codes-de-calcul/Pages/Le-logiciel-de-calcul-ISIS-4576.aspx#.

[31] S. Suard, C. Lapuerta, F. Babik, and L. Rigollet, "Verification and validation of a CFD model for simulations of large-scale compartment fires," *Nuclear Engineering and Design*, vol. 241, no. 9, pp. 3645–3657, 2011.

[32] C. Lapuerta, S. Suard, F. Babik, and L. Rigollet, "Validation process of ISIS CFD software for fire simulation," *Nuclear Engineering and Design*, vol. 253, pp. 367–373, 2012.

[33] P. J. Jones and G. E. Whittle, "Computational fluid dynamics for building air flow prediction-current status and capabilities," *Building and Environment*, vol. 27, no. 3, pp. 321–338, 1992.

[34] P. J. Roache, "Quantification of uncertainty in computational fluid dynamics," *Annual Review of Fluid Mechanics*, vol. 29, pp. 123–160, 1997.